Collective Hypersonic Excitations in Strongly Multiple Scattering Colloids

T. Still,[1] G. Gantzounis,[2] D. Kiefer,[3] G. Hellmann,[3] R. Sainidou,[4] G. Fytas,[1,5] and N. Stefanou[6]

[1]*Max Planck Institute for Polymer Research, Ackermannweg 10, 55128 Mainz, Germany*
[2]*Institute of Microelectronics, NCSR "Demokritos," 15310 Athens, Greece*
[3]*Deutsches Kunststoff-Institut, Schlossgartenstraße 6, 64289 Darmstadt, Germany*
[4]*Laboratoire Ondes et Milieux Complexes FRE CNRS 3102, Université du Havre, 76610 Le Havre, France*
[5]*Department of Materials Science, University of Crete and FORTH, 71110 Heraklion, Greece*
[6]*Section of Solid State Physics, University of Athens, Panepistimioupolis, 15784 Athens, Greece*

(Received 21 October 2010; revised manuscript received 15 December 2010; published 29 April 2011)

Unprecedented low-dispersion high-frequency acoustic excitations are observed in dense suspensions of elastically hard colloids. The experimental phononic band structure for SiO_2 particles with different sizes and volume fractions is well represented by rigorous full-elastodynamic multiple-scattering calculations. The slow phonons, which do not relate to particle resonances, are localized in the surrounding liquid medium and stem from coherent multiple scattering that becomes strong in the close-packing regime. Such rich phonon-matter interactions in nanostructures, being still unexplored, can open new opportunities in phononics.

DOI: 10.1103/PhysRevLett.106.175505 PACS numbers: 82.70.Dd, 43.20.+g, 61.46.−w, 62.60.+v

In structured materials with spatial variation in their elastic properties, i.e., density ρ, longitudinal and transverse sound velocities, c_l and c_t, the propagation of acoustic waves can be distinctly different from the wave propagation in the isotropic bulk material. The most prominent paradigm is a phononic crystal that can exhibit, under certain conditions, acoustic band gaps, i.e., regions of frequency for which propagation of acoustic waves is forbidden within the crystal. So far, two mechanisms are reported for band gap opening in phononic crystals as shown schematically in Fig. 1(a): (a) Bragg band gaps for wave propagation vectors at an edge or at the center of the Brillouin zone due to destructive interference between incident and scattered acoustic waves, when the sound wavelengths commensurate the structure periodicity. Audible sound is modified by meter-sized structures [1], while sub-μm lattices interact with hypersonic (GHz) frequencies [2]. (b) Hybridization gaps due to the anticrossing interaction between the extended acoustic band and narrow bands originating from the resonant modes of the individual building units [2–6]. These are analogous to the well-known *s*-*d* hybridization gaps in the electron band structure of transition metals [7]. Polymer-based periodic structures such as 1D periodic stacks of alternating nanolayers [8,9] and 2D triangular arrays of cylindrical holes [10] exhibit only Bragg band gaps. In contrast, colloid-based nanostructures, such as colloidal crystals, prove a much more versatile system for engineering phonon dispersion due to both the rich chemistry of the individual particles, which allows the facile tuning of the elastic parameters over a wide range, as well as their ability to self-assemble [11,12]. For example, a single hypersonic Bragg band gap was realized in self-assembled face-centered cubic (fcc) crystals of elastically soft (polymer) colloids at a volume fraction $\phi = 0.74$ [2] and relatively low elastic impedance ($Z = \rho c_l$) contrast (ΔZ) between the colloids and the surrounding matrix. More interestingly, in such soft colloidal systems with larger ΔZ, the second mechanism of a hybridization band gap, for which structure periodicity is not a precondition [5], is activated within the same frequency region. An increase in ΔZ results in a gradual evolution of the known band gaps [2,5].

Herein we report on unprecedented collective hypersonic excitations in phononic structures based on elastically hard silica colloids. The band diagram, recorded by Brillouin light scattering (BLS) at high volume fraction in an index-matching liquid, is found to be qualitatively different from that of softer (polymer-based) colloidal systems as a result of a further boosted ΔZ. Full-elastodynamic calculations ascribe the unexpected wave dispersion to the strong phonon multiple scattering, which becomes the dominant mechanism at the highest volume fraction.

We investigate colloidal systems based on three species of SiO_2 spheres with diameter $d = 192$, 354, and 632 nm and low size polydispersity ($< 5\%$) [11]. These were synthesized by Stoeber process in ethanol/ammonia bearing no stabilizing layer. The colloidal particles were transferred into an ethoxy-ethoxyethyl acrylate (SR256, Sartomer) isorefractive liquid matrix at $\phi \approx 0.35$; i.e., multiple light scattering was strongly suppressed. The colloids were pushed beyond the equilibrium colloidal crystal ($\phi \approx 0.54$) to dense packed fcc polycrystalline lattice by ultracentrifugation (7000 g) in standard NMR tubes [13]. This was supported by static light scattering and the opalescence of the samples (see supplemental material [14]). Twinning in the fcc structure would not influence our general conclusions. For comparison, an analogous structure based on soft poly(methyl methacrylate) (PMMA)

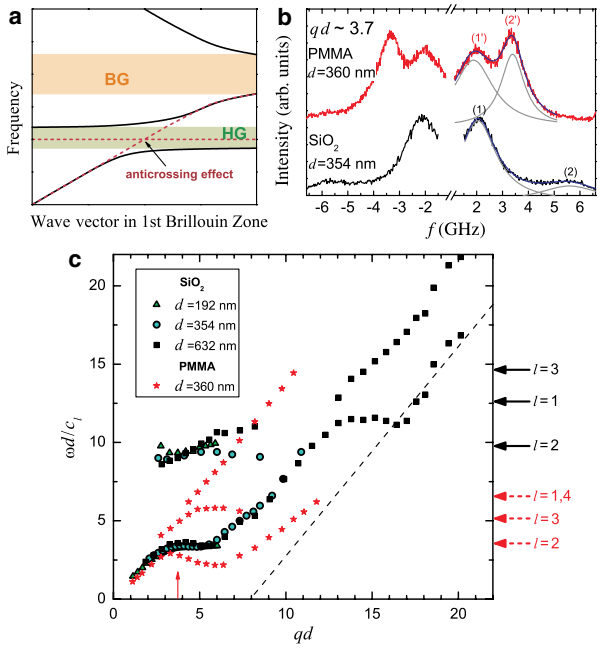

FIG. 1 (color online). (a) Schematic band structure in phononic crystals of elastic soft colloids [2,5] (BG, Bragg gap; HG, hybridization gap). (b) Exemplary spectra for polycrystalline colloidal suspensions of close-packed SiO_2 spheres in SR256 and PMMA spheres in decaline-tetraline, of diameter d, at $qd \approx 3.7$ [vertical arrow in band diagram (c)]. The solid lines on the anti-Stokes side of the spectra show the fits of a double Lorentzian. (c) Reduced phononic band diagram deduced from BLS experiments on the two systems and three different d for SiO_2/SR256. For the largest d, the dashed line represents the first Bloch harmonic intersecting the abscissa at $qd \approx 8$. The positions of the resonant lth multipole modes of the single SiO_2 (solid arrows) and PMMA (dashed arrows) spheres immersed in the corresponding liquid matrices are indicated on the right margin.

spheres ($d = 360$ nm), sterically stabilized with polyhydrostearic acid, was prepared in an isorefractive matrix. The band diagrams were recorded by BLS [2], with the probing wave vector $\mathbf{q}$ scanned by changing the scattering angle θ, i.e., $q = \frac{4\pi n}{\lambda} \sin\frac{\theta}{2}$, where $n(= 1.44$ for SR256) is the refractive index and $\lambda = 532$ nm the laser wavelength. At each q, BLS records the spectrum, $I(q, \omega)$ (angular frequency $\omega = 2\pi f$), whose spectral shape is represented by Lorentzian line shapes convoluted with the instrument function as seen in the anti-Stokes side of $I(q, \omega)$ in Fig. 1(b) (solid lines) for both colloidal systems. At the same dimensionless wave number qd, the spectra are distinctly different. For SiO_2/SR256 only one acoustic peak (1) is found followed by a very weak signal (2) at the first particle resonance frequency (with multipole order $l = 2$ at $f = 6$ GHz). On the contrary, PMMA/decaline-tetraline shows a clear splitting of the signal ($1' + 2'$) due to a hybridization gap at the frequency of the corresponding first resonance ($l = 2$) [5]. The latter appears at a lower frequency than in SiO_2 due to the softer nature of the PMMA particles.

Figure 1(c) displays the experimental dispersion relation $\omega(q)$ in the polycrystalline colloidal suspensions of close-packed SiO_2 spheres with different diameters. The three dispersion diagrams are plotted in reduced frequency $\omega d/c_l$, where c_l is the sound velocity in the host liquid, versus qd, so that the dispersion remains valid for any sphere size. Indeed, all three experimental dispersions follow the same reduced band diagram. At low frequencies and low q's, there is only one longitudinal acoustic phonon branch [15]. Contrary to other studies on sintered SiO_2 opals [16], transverse phonons are not observed since shear waves are not supported in the absence of consolidation of neighboring particles. In a phononic crystal, the bands are repeated periodically if we add a reciprocal-lattice vector $\mathbf{G}$. In fact, the experimental dispersion at $qd > 17$ reveals the presence of the first Bloch harmonic [dashed line in Fig. 1(c)], supporting the polycrystalline structure of the sample. It is shifted by $qd \approx 8$ in agreement with the dimensionless shortest reciprocal-lattice distance $G_{\min}d$. Counterintuitively, the intensity of this mode at $\omega(\mathbf{q} + \mathbf{G})$ in the BLS spectrum (not shown) is stronger than the acoustic (first order) phonon $\omega(\mathbf{q})$ [17].

For comparison, Fig. 1(c) also displays the experimental band structure of the PMMA colloidal suspension. The polycrystalline suspension of hard SiO_2 displays distinctly different band diagrams from both poly- and single-domain colloidal crystals of soft polymer spheres [2]. The coherence of the structure is manifested in the shape of the band structure of the latter, and no Bragg band gap (as found in single-domain opals [5]) is observed in multi-domain crystals. In the case of close-packed SiO_2, however, the dispersion is insensitive to the polycrystallinity, as indicated by the virtually identical band diagram for a single crystalline infiltrated silica opal in the accessible (smaller) q range [14]. The lack of superposition for the band diagrams of the two colloidal systems relates to the evolution of the fundamental acoustic branch with qd. For SiO_2 colloids, it bends near an edge of the first Brillouin zone exhibiting a low dispersion beyond $qd = 3.5$. It then continues at higher frequencies but shifted at larger qd (≈ 6) values with respect to the extrapolation of the low-frequency acoustic branch. The band diagram of the suspension of the soft (PMMA) colloids is distinctly different. The fundamental acoustic branch continues beyond the hybridization gap at $\omega d/c_l \approx 3.5$ ($l = 2$) and the weak localized mode at $\omega d/c_l \approx 6$ ($l = 3$). Thus the different shape of the band diagram and the plateau about $\omega d/c_l \approx 3.5$ are intrinsic features of the hard colloidal suspension.

The oscillations of the individual scatterers (particles) play an important role in the wave propagation in colloidal structures. A single spherical particle in vacuum exhibits purely transverse (torsional) and mixed longitudinal-transverse (spheroidal) vibrational eigenmodes [18–21]. When the particle is embedded in the liquid solvent, each spheroidal eigenmode is coupled with the acoustic field in the solvent and, consequently, energy leaks out of the sphere. As a result, the eigenmode acquires a finite lifetime

and from a bound state becomes a resonant mode. In the colloidal structure, the resonant modes of neighboring particles couple weakly with each other through the acoustic field in the liquid solvent, thus forms a band of collective propagating modes, which have a large amplitude inside each particle. This band extends over a narrow frequency region near the eigenfrequency of the corresponding single-particle mode. Such narrow bands of resonant modes—and consequent hybridization gaps—appear in suspensions of soft-particle colloids [5]. Figure 1(c) shows the three lower resonance frequencies (arrows) of the PMMA particle in liquid; the lowest $l = 2$ mode is responsible for the first gap in the band diagram of this system. For the hard SiO_2 spheres, the resonance modes, and hence the resulting narrow bands, are pushed to higher frequencies, $\omega d/c_l > 9.5$. The observed fundamental resonance band, associated with quadrupole particle modes, appears close to the corresponding single-particle resonance at $\omega d/c_l \approx 10$. The unexpected plateau at $\omega d/c_l \approx 3.5$ of the dispersion diagram of the SiO_2/SR256 system is most likely the fingerprint of a narrow band, which cannot be ascribed to any localized resonant mode of the individual particles. It is worth noting that similar narrow bands have been encountered in the phononic band diagram of dry SiO_2 opals, but, so far, defied convincing full interpretation [22].

The theoretical phononic band structure of the SiO_2 colloidal crystals in SR256 matrix is rigorously computed by the layer-multiple-scattering method [23]. The input parameters for SiO_2 and SR256, respectively, are $\rho = 1900$ and 1013 kg/m^3, $c_l = 4420$ and 1420 m/s, $c_t = 2780$ and 0 m/s. Using an angular-momentum cutoff $l_{\max} = 8$ and considering 85 2D reciprocal-lattice vectors in the relevant spherical-wave and plane-wave expansions, respectively, ensures very good convergence of the results (better than 1%). The calculated nondegenerate phononic bands, which are the only acoustically active bands along the [111] and [001] fcc directions [4], are shown in Fig. 2 in the repeated zone scheme. It can be seen that the experimental data nicely follow the principal longitudinal acoustic branch (1) and the narrow band (2). It is also worth noting that no frequency gap is observed experimentally, presumably because of the polycrystalline nature of the samples; the gaps shown for [111] and [001] are not omnidirectional as verified by detailed numerical calculations. The band structure of Fig. 2 originates from the interaction between the principal acoustic branch and the narrow band (2). The experimental data beyond the plateau ($qd > 6$) follow higher frequency bands, which deviate from the extrapolation of the low-frequency acoustic branch because of strong band bending.

Experimentally, the narrow band (2) is observed only at the close-packing ratio; it is absent at $\phi \approx 0.35$ and $\phi \approx 0.54$. This band might therefore originate from localized torsional eigenmodes of the SiO_2 particles that form a narrow band of propagating Bloch modes. However, as already mentioned, mere touching of the particles without

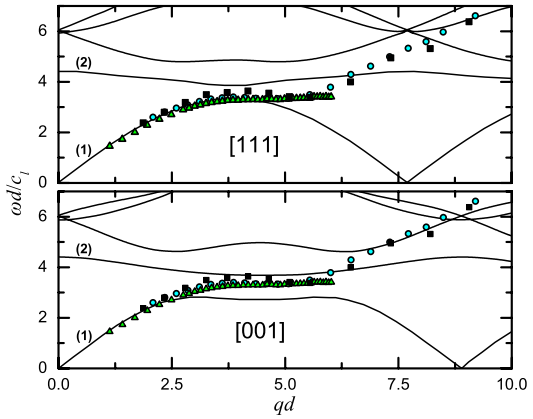

FIG. 2 (color online). Phononic band structure (only nondegenerate bands are shown) of a fcc crystal of closely packed SiO_2 spheres in SR256 along its [111] and [001] directions. The triangles, circles, and squares show the experimental results for the corresponding samples in Fig. 1. The longitudinal acoustic branch is indicated by (1) and the flat band by (2).

tangential interactions cannot allow propagation of a shear displacement field. Moreover, the torsional eigenfrequencies of an elastic sphere are too high [18]. The lowest fundamental frequency is at $\omega d/c_l \approx 9.8$, which is well above the flat band (2). In another scenario, the band (2) might stem from resonant modes of cavities formed between close-packed SiO_2 spheres with liquid filling up the empty spaces. Though the shape of these cavities is rather complex, a rough estimate of the fundamental resonance frequency can be made by assuming volume-filling spherical cavities with diameter $d_c = [(1 - \phi)/\phi]^{1/3} d$ with $\phi = 0.74$. Applying the standing-wave condition $d_c = \lambda/2$, we obtain $\omega d/c_l \approx 4.4$, which is in good agreement with the position of the flat band. However, these cavities are not closed to justify application of the above standing-wave condition, but rather form a continuous network. In addition, the theoretical calculations (see Fig. 3) show that the frequency of the narrow band (2) increases with decreasing ϕ. This is in clear contrast to the opposite trend anticipated on the basis of the fluid-cavity model.

In order to gain more insight into the formation of the narrow band in question and the lack of superposition for the two systems in Fig. 1(c), we carried out systematic calculations by progressively increasing the diameter of the SiO_2 spheres, centered at the sites of a given fcc lattice of lattice constant a in a SR256 matrix, from 0 (empty lattice) to $a_0 = a\sqrt{2}/2$ (close-packed spheres). In the empty-lattice limit, the phonon dispersion diagram is that of a homogeneous medium in the reduced-zone scheme (Fig. 3). This is given by $\omega = c_l|\mathbf{q} + \mathbf{G}|$, where $\mathbf{G} = \frac{2\pi}{a} \times (n_1, n_2, n_3)$ are fcc reciprocal-lattice vectors. The diagram with the lowest bands corresponding to the above $\mathbf{G}$ vectors along the Γ-L direction, i.e., for $\mathbf{q} = \frac{2\pi}{a}(\xi, \xi, \xi)$, $0 \leq \xi \leq 1/2$, is shown in Fig. 3. The perturbation induced when actual scatterers occupy the lattice sites removes the high degeneracy of the empty-lattice bands. Each of

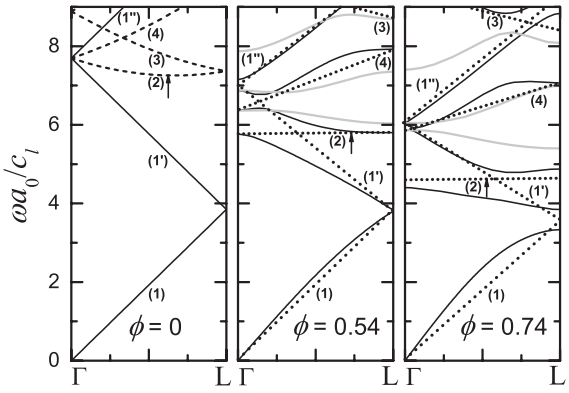

FIG. 3. Phononic band structure of SiO_2/SR256 fcc crystals with $\phi = 0$, $\phi = 0.54$, and $\phi = 0.74$ along their [111] (Γ-L) direction. The flat band of interest is indicated by an arrow. For $\phi = 0$, the solid and dashed lines denote nondegenerate and threefold degenerate bands, respectively, corresponding to reciprocal-lattice vectors (in units $2\pi/a$): (1): $(0, 0, 0)$; (1′): $(-1, -1, -1)$; (1″): $(1, 1, 1)$; (2): $(1, -1, -1)$, $(-1, 1, -1)$, $(-1, -1, 1)$; (3): $(0, 0, -2)$, $(0, -2, 0)$, $(-2, 0, 0)$; (4): $(-1, 1, 1)$, $(1, -1, 1)$, $(1, 1, -1)$. For $\phi = 0.54$ and $\phi = 0.74$, the black and gray solid lines denote the actual nondegenerate and doubly degenerate bands, respectively. Dotted lines show schematically the nondegenerate bands that would be in the absence of anticrossing interaction, with the corresponding number denoting their origin in the empty-lattice ($\phi = 0$) diagram.

the threefold degenerate branches of the dispersion diagram ($\phi = 0$) along Γ-L splits into one nondegenerate (black solid lines) and one doubly degenerate (gray solid lines) band. Interestingly, there are no additional bands apart from those appearing in the empty-lattice dispersion diagram ($\phi = 0$). We note that similar dispersion diagrams are obtained for the same lattice with ideally hard spheres, which, by definition, have no resonant modes; the wave field is expelled at any frequency from the interior of such spheres.

As seen in Fig. 3, the nondegenerate flat band, indicated by an arrow, splits off a threefold degenerate dispersion branch of the empty lattice and is progressively shifted down to lower frequencies with increasing the particle diameter. Concurrently, its character changes from extended to more localized within fluid regions [24]. Anticrossing interaction, which takes place between bands of the same symmetry, finally leads to the band diagrams shown by the black and gray solid lines in Fig. 3; absence of anticrossing interaction (bare Bragg scattering) would lead to the dotted lines in Fig. 3 for finite ϕ. Thus, the formation and evolution of the flat band in the dense suspension of hard colloids should be understood as a multiple-scattering effect rather than a tight-binding-like process from localized single-particle or single-cavity modes. It is also worth noting that the presence of the flat band near a Bragg point leads to sizable gaps due to the superposition of Bragg scattering and anticrossing interaction, as well as to large band bending as a result of strong band mixing (see, e.g., at $\omega a_0/c_l \approx 6$ for $\phi = 0.54$ and $\omega a_0/c_l \approx 4$ for $\phi = 0.74$ in Fig. 3). Otherwise, the Bragg gaps are relatively small and not discernible in Fig. 3 (dotted lines).

The phonon dispersion diagram of dense SiO_2 colloids exhibits novel and unexpected features in view of the current state of the art based on elastically soft colloids. Full-elastodynamic calculations with no adjustable parameter represent well the experimental band structure and provide consistent interpretation of the underlying mechanisms distinct in the present system. Apart from the extended effective-medium band and narrow bands stemming from localized particle resonances at relatively high frequencies, we identified additional almost dispersionless collective modes at lower frequencies. These originate from strong coherent multiple scattering and are localized in regions of the liquid matrix. Strong mode hybridization leads to large band bending while directional gaps arise from the superposition of Bragg scattering and anticrossing interaction. Therefore, dense suspensions of elastically hard colloids exhibit unique features that enrich the opportunities for phononic band engineering, controlling heat propagation, and tailoring the phonon-matter interaction in nanostructures.

DFG is acknowledged for financial support.

[1] R. Martinez-Salazar *et al.*, Nature (London) **378**, 241 (1995).
[2] W. Cheng *et al.*, Nature Mater. **5**, 830 (2006).
[3] Z. Y. Liu *et al.*, Science **289**, 1734 (2000).
[4] I. E. Psarobas *et al.*, Phys. Rev. B **65**, 064307 (2002).
[5] T. Still *et al.*, Phys. Rev. Lett. **100**, 194301 (2008).
[6] V. Leroy *et al.*, Appl. Phys. Lett. **95**, 171904 (2009).
[7] W. A. Harrison, *Solid State Theory* (Dover, New York, 1980).
[8] N. Gomopoulos *et al.*, Nano Lett. **10**, 980 (2010).
[9] P. M. Walker *et al.*, Appl. Phys. Lett. **97**, 073106 (2010).
[10] T. Gorishnyy *et al.*, Appl. Phys. Lett. **91**, 121915 (2007).
[11] T. Still *et al.*, Nano Lett. **8**, 3194 (2008).
[12] M. Grzelczak *et al.*, ACS Nano **4**, 3591 (2010).
[13] J. Wijnhoven and W. L. Vos, Science **281**, 802 (1998).
[14] See supplemental material at http://link.aps.org/supplemental/10.1103/PhysRevLett.106.175505 for sample characterization and comparison to single domain opals.
[15] D. O. Riese and G. H. Wegdam, Phys. Rev. Lett. **82**, 1676 (1999).
[16] A. V. Akimov *et al.*, Phys. Rev. Lett. **101**, 033902 (2008).
[17] R. J. P. Engelen *et al.*, Nature Phys. **3**, 401 (2007).
[18] H. Lamb, Proc. London Math. Soc. **s1-13**, 189 (1882).
[19] R. S. Penciu *et al.*, Phys. Rev. Lett. **85**, 4622 (2000).
[20] M. H. Kuok *et al.*, Phys. Rev. Lett. **90**, 255502 (2003).
[21] T. Still *et al.*, J. Phys. Chem. Lett. **1**, 2440 (2010).
[22] R. Sainidou *et al.*, Z. Kristallogr. **220**, 848 (2005).
[23] R. Sainidou *et al.*, Comput. Phys. Commun. **166**, 197 (2005).
[24] J. D. Joannopoulos *et al.*, *Photonic Crystals: Molding the Flow of Light* (Princeton University Press, Princeton, 2008), 2nd ed.